

Deep structure and origin of the Baikal rift zone

Dapeng Zhao ^{a,*}, Jianshe Lei ^a, Tomofumi Inoue ^a, Akira Yamada ^a, Stephen S. Gao ^b

^a *Geodynamics Research Center, Ehime University, Matsuyama 790-8577, Japan*

^b *Department of Geology, Kansas State University, Manhattan, KS 66506, USA*

Received 28 May 2005; received in revised form 11 January 2006; accepted 17 January 2006

Available online 21 February 2006

Editor: S. King

Abstract

P-wave velocity images are determined under the Baikal rift zone in Siberia by using teleseismic tomography. Our results show prominent low-velocity anomalies in the upper mantle under the Baikal rift zone and high-velocity anomalies in the lithosphere under the Siberian craton. The low-velocity anomalies are interpreted as a mantle upwelling (plume) which has played an important role in the initiation and evolution of the Baikal rift zone. The rift formation may be also controlled by other factors such as older (prerift) linear lithosphere structures favorably positioned relative to the upwelling and favorable orientation of the far-field forces caused by the India–Asia collision.

© 2006 Elsevier B.V. All rights reserved.

Keywords: Baikal rift zone; teleseismic tomography; mantle upwelling; plume; India–Asia collision

1. Introduction

The Baikal rift zone is composed of a branched chain of Late Cenozoic half-grabens extending over a distance of about 1500 km in Siberia [1–3] (Fig. 1). It is situated at the boundary of the Siberian platform (craton) to the north-west and the Mongolian fold belt to the south-east. Lake Baikal occupies only about a third of the rift zone. It is the deepest lake (1620 m) in the world and contains 20% of the world's fresh water [4]. The Baikal rift zone is characterized by high surface heat flow, flanking normal faults, and lower upper mantle velocity [5–7]. The 1500 km echelon system of rift depressions is the most seismically active continental rift in the world. During the past 280 yrs, 13

earthquakes with magnitudes larger than 6.5 have occurred within this area [8]. The Baikal rift is more than 2000 km away from the nearest active plate boundary, and hence it is well suited to study the intracontinental rifting.

The Baikal rift is probably the most debated of all rifts in terms of its origin. Most Russian scientists support the active rift hypothesis that theorizes an anomalous upper mantle formed beneath the continental lithosphere and led to the development of the rift (e.g., [2,4,6,7,9]). The passive hypothesis suggests the rift began as a result of the collision of India with Asia [1,3,10–12]. Several recent studies suggested the possibility of a mixture of several effects, giving a rather complex evolutionary picture (e.g., [13–15]). These disagreements are mainly caused by the fact that the deep structure of the Baikal rift zone has not been understood well [6], although many researchers have studied the crust and upper mantle structure under this region using various

* Corresponding author. Tel.: +81 89 927 9652.

E-mail address: zhao@sci.ehime-u.ac.jp (D. Zhao).

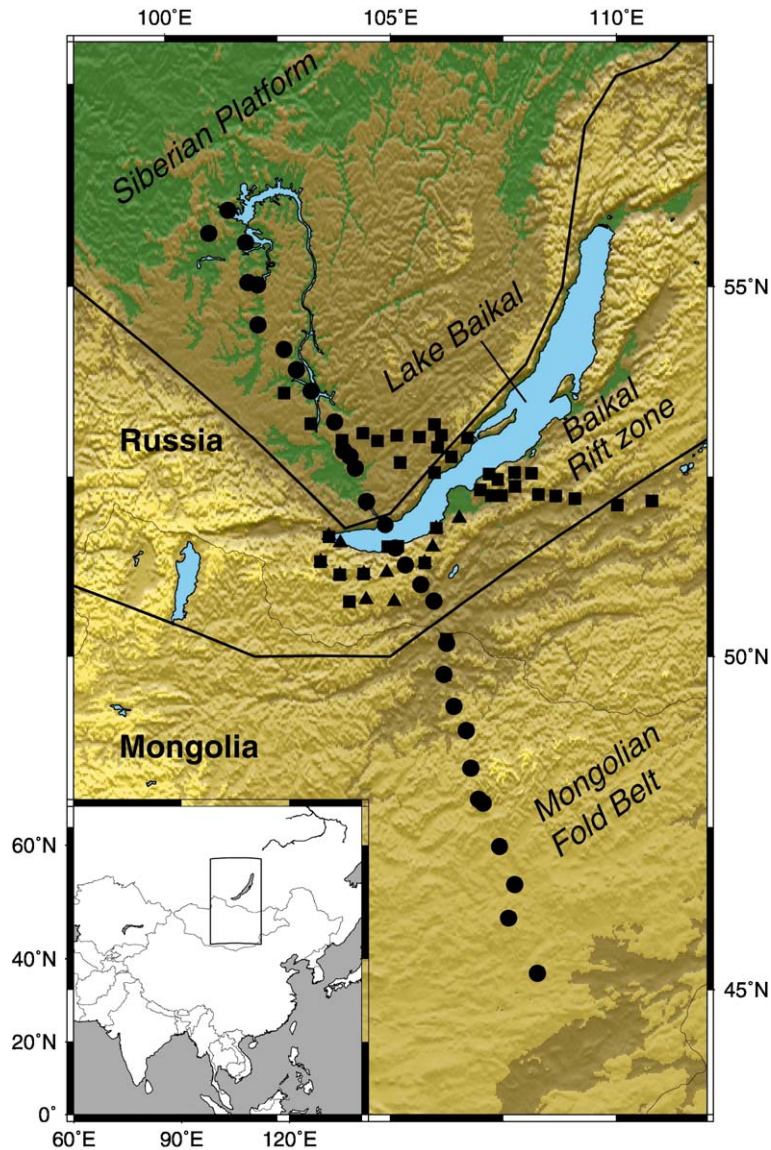


Fig. 1. Map of the study area. Solid squares show the locations of 36 portable seismic stations deployed by University of California (UC) and University of Wisconsin (UW) during July to October 1991. Solid circles and triangles denote 28 portable stations deployed by UC and 12 portable stations installed by UW, respectively, during July to September 1992. The two curved lines show the approximate boundaries between the Siberian craton, the Baikal rift zone and the Mongolian fold belt [42]. Insert shows the location of the present study area.

geophysical methods including seismic tomography (e.g., [4,6,7,9,16–19]).

In this work, we carefully collected a large number of high-quality arrival time data from original seismograms of teleseismic events recorded by a portable seismic network and used a modified tomographic inversion method. A tomographic image of the upper mantle under the Baikal region is obtained, which sheds new light on the deep structure and origin of the Baikal rift zone.

2. Data and method

We used 76 portable seismic stations from two PASSCAL (Program for Array Seismic Studies of the Continental Lithosphere) experiments conducted during July to October 1991 and July to September 1992 by a field team from the Institute of Earth's Crust, Irkutsk, University of Wisconsin, and University of California at Los Angeles [4,7,18]. These stations were equipped with short-period, three-component seismographs and

were deployed in and around the Baikal rift zone (Fig. 1). Note that a few stations were deployed at almost the same sites in the southwestern part of Lake Baikal during the 1991 and 1992 experiments (Fig. 1). We used 710 first P arrivals from 79 teleseismic events recorded by the 36 portable stations in 1991, which were collected by Gao et al. [4] (Figs. 1 and 2). In this work, we newly picked 1072 first P arrivals from seismograms of 63 teleseismic events recorded by the 40 portable stations deployed in 1992. These events have epicentral distances of 25 to 95 degrees and magnitudes larger than M 4.9 (Fig. 2). Only seismograms with a clear onset were used, and those from an event were not used if the number of high-quality arrival time picks was less than 8. Combining the 1991 and 1992 data sets, we have a total of 1782 first P-wave arrivals from 142 teleseismic events recorded by 76 portable stations (Figs. 1 and 2). Hypocentral parameters of the 142 events redetermined accurately by Engdahl et al. [20] were used in this study. The 1782 rays crisscross well in both the horizontal and vertical directions down to 700km depth (Fig. 3).

Theoretical arrival times were calculated by using the iasp91 Earth model [21]. Residuals were found by subtracting these theoretical arrival times from observed ones, and relative residuals were formed for each event by subtracting the event's mean residual from the raw residuals [22,23]. Distribution of average relative

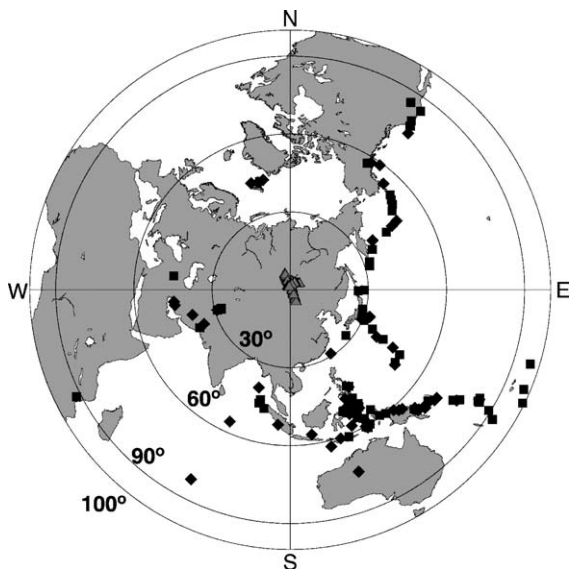


Fig. 2. Epicentral locations of the 79 teleseismic events recorded in 1991 (solid squares) and 63 events recorded in 1992 (solid diamonds), which are used in this study. The gray triangles denote the portable seismic stations deployed in and around the Baikal rift zone in 1991 and 1992.

residuals at each of the stations reflects the lateral heterogeneity under the seismic network (Fig. 4). Large early arrivals at stations north of Lake Baikal reflect the cold and thick lithosphere under the Siberian craton. Large delayed arrivals are visible about Lake Baikal, suggesting the existence of significant low-velocity materials under the rift zone. Minor to moderate early and delayed arrivals appear at stations south of Lake Baikal, which reflect the complex structural variations under the Mongolian fold belt [7,19].

To invert the relative travel time residuals for the three-dimensional (3-D) velocity structure under the study area, we used an updated version of the tomographic inversion method [23,24]. A 3-D grid was set up in the study area; the velocity perturbations from the 1-D iasp91 Earth model [21] at the grid nodes were taken as unknown parameters. The velocity perturbation at any point in the model was computed by interpolating the velocity perturbations at the eight grid nodes surrounding that point. A 3-D ray tracing technique was used to compute travel times and ray paths [25,26]. The large and sparse system of observation equations that relate the observed relative residuals to the unknown velocity parameters was resolved by using a conjugate-gradient algorithm [27] with damping and smoothing regulations [24,28], similar to the previous tomographic studies [29–31]. We made detailed analyses of the trade-off between data variance reduction and model norm and selected the final 3-D velocity model based on the result of the trade-off analyses. The station elevations were taken into account in the 3-D ray tracing and inversion.

Note that several studies have investigated the 3-D velocity structure of the Baikal rift zone using the teleseismic arrival time data recorded by the 1991 and 1992 seismic experiments [4,7,12]. Gao et al. [4] used the 1991 data set to determine the geometry of the lithosphere–asthenosphere boundary. Gao et al. [7] used data from 28 stations in 1992 to determine the 3-D velocity structure with the ACH method [32]. Achauer and Masson [12] applied the ACH method to the 1991 and 1992 data sets collected by Gao et al. [4,18]. In comparison with the previous studies, we have used an improved data set from all the available stations deployed in 1991 and 1992 and applied an updated tomographic method as mentioned above.

3. Analysis and results

Teleseismic tomography cannot determine the 3-D crustal structure well because the teleseismic rays arrive at stations nearly vertically and so they do not crisscross

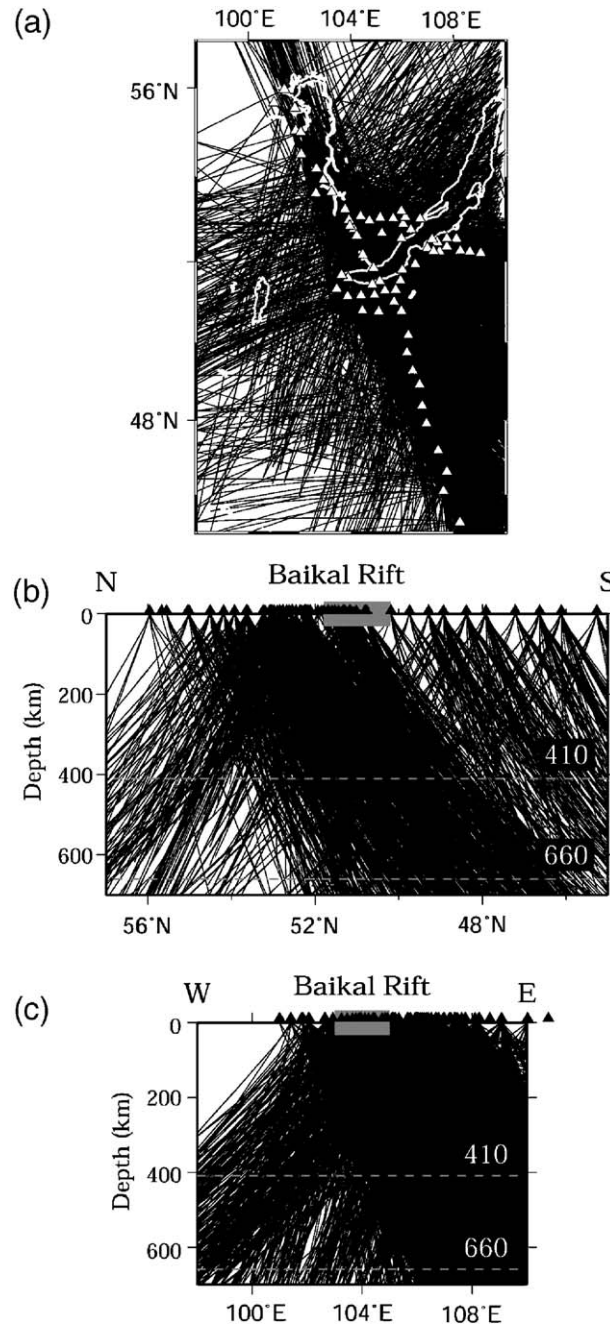


Fig. 3. Distribution of the 1782 teleseismic rays used in this study in plan view (a) and in north–south (b) and east–west (c) vertical cross-sections. Triangles denote the seismic stations used. The bold bar in panels (b) and (c) denotes the location of the Baikal rift zone.

near the surface. Hence it is necessary to correct the teleseismic relative residuals for the heterogeneous crustal structure (e.g., [31,33]). In this work we used two 3-D crustal velocity models to make the crustal corrections. One is the model CRUST2.0 [34] which is an updated version of CRUST5.1 [35] and is specified on a 2×2 degree grid for the lateral velocity variations

of the crust and Moho topography. The other is a 3-D crustal model derived from a receiver function analysis [36] of the same teleseismic waveform data used in this study. We conducted many tomographic inversions using different grids. The spacing between grid nodes ranges from 0.5 to 2 degrees laterally and 50 to 200 km in depth. Inversions were also performed by using

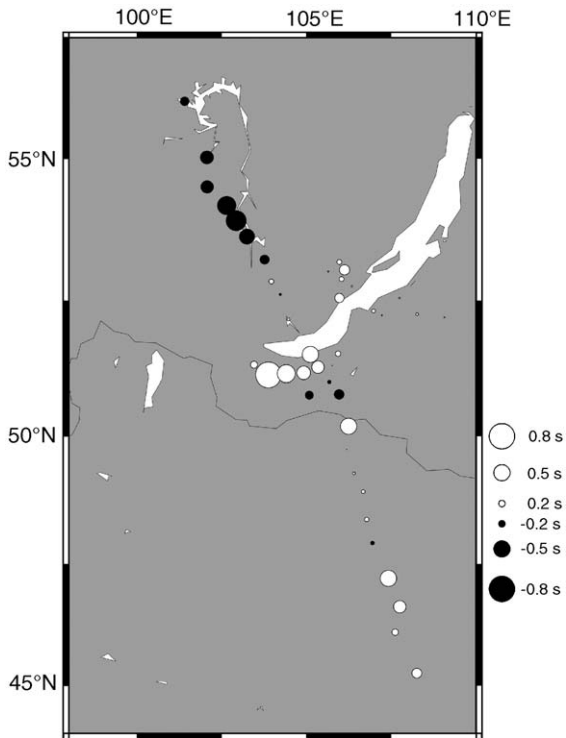


Fig. 4. Distribution of average relative residuals at each of the seismic stations. Solid and open circles denote early and delayed arrivals, respectively. The scale for the residuals is shown on the right. The curved line denotes the national boundary between Russia and Mongolia.

various damping and smoothing parameters, and different starting velocity models. The pattern of the tomographic images is generally stable, although there are slight changes in the amplitude of the velocity anomalies.

Figs. 5 and 6 show our optimal tomographic model based on the trade-off between the data variance reduction and model norm as well as detailed resolution analyses which are described in the following. The model CRUST2.0 was used to make the crustal corrections (Figs. 5 and 6). Fig. 7a shows the tomographic result with the crustal corrections using the model [36]. The crustal corrections to the teleseismic residuals range from 0.05 to 0.35 s. The two tomographic models using different crustal corrections are quite similar to each other (Figs. 6a and 7a). A prominent low-velocity (low-V) anomaly is visible beneath the Baikal rift zone from the Moho down to about 300 km depth, then it connects with a smaller low-V zone at depths of 300–600 km under the southern edge of the Siberian craton (Figs. 6a and 5d). The low-V zone looks more continuous in Fig. 7a. High-velocity (high-V) anomalies exist under the Siberian craton

down to about 180 km depth (Figs. 6a, 7a). Both high-V and low-V anomalies exist in the lithosphere of the Mongolian fold belt (Figs. 5a, b, 6a, and 7a). It is known that the Mongolian fold belt exhibits complex geological structures [3,6,13,19].

To confirm the main features of the tomographic result, we conducted detailed resolution analyses. A direct way to evaluate the resolution of a tomographic result is to calculate a set of travel time delays that result from tracing the corresponding rays through a synthetic structure as though they are data, and then to compare the inversion result with the initial synthetic structure. In the synthetic tests, the numbers of stations, events and ray paths are the same as those in the real data set. In this work we conducted three kinds of resolution tests [23,25]. The first is the synthetic tests for examining the resolvability of the structure right beneath the Baikal rift zone (Fig. 8). The second is checkerboard resolution tests for evaluating the spatial resolution of tomographic images in the entire study area (Fig. 9). The third is a restoring resolution test [25] (Fig. 7b) for the obtained tomographic model (Fig. 7a). In all of the tests, random errors having a normal distribution with a standard deviation of 0.1 s were added to the synthetic data, and the same inversion algorithm as that for the real data was used.

Fig. 8 shows the results of three synthetic tests of the low-V anomalies beneath the Baikal rift. In these tests a slow anomaly of up to 2% is put in the synthetic model from the surface down to 200, 400 and 600 km depth, respectively (Fig. 8a, c, e). After the inversions, the slow anomalies are well recovered with little smearing in the horizontal and depth directions (Fig. 8b, d, f).

The checkerboard resolution test is just a special form of a synthetic test. The only difference between them is in the input model. To make a checkerboard, positive and negative velocity perturbations (2%) are assigned to the 3-D grid nodes that are arranged in the modeling space, the image of which is straightforward and easy to remember. Therefore, by just examining the inverted images of the checkerboard, one can easily understand where the resolution is good and where it is poor. In this work, we performed many such tests by adopting different grid spacings and found that the optimal grid spacing for the tomographic inversion of our data set is 2 degrees in the horizontal direction and 50 to 200 km in depth (Fig. 9). The test results show that the checkerboard pattern is well recovered for all depth levels in and around the Baikal rift zone (Fig. 9). The spatial resolution is reduced in the mantle transition zone, compared with that in the upper mantle down to 400 km depth (Figs. 8 and 9).

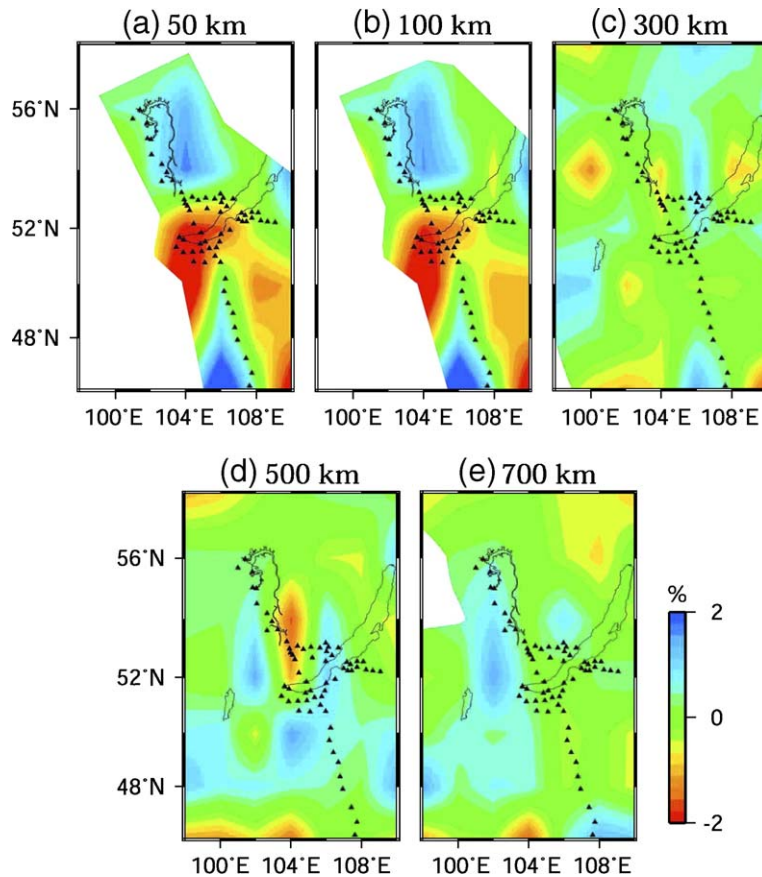


Fig. 5. Plan views of P-wave velocity images obtained in this study. The layer depth is shown above each map. Red and blue colors denote slow and fast velocities, respectively. The velocity perturbation scale is shown on the right. Solid triangles denote the locations of the portable seismic stations.

The restoring resolution test [25] is also a special form of a synthetic test. In this test the obtained tomographic image (Fig. 7a) was taken as the input model. The inverted result (Fig. 7b) shows that the low-V zone under the Baikal rift zone is well recovered. Through these synthetic tests, we believe that the main features of the tomographic result (Figs. 6a and 7a) are reliably resolved by our data set and inversions, although the resolution of the tomographic images in and below the mantle transition zone is reduced. Because of the geometry of the seismic array used (Fig. 1) our tomographic images have a good resolution in the NW–SE direction but a poor resolution in the SW–NE direction.

4. Discussion

Gao et al. [4,7] used the teleseismic data recorded by the same portable seismic array to invert for the geometry of the lithosphere–asthenosphere boundary (LAB) beneath the Baikal rift zone. They found that the

LAB upwarps under the rift, and the upwarp has an asymmetric shape. It was further found that the LAB downwarps on either side of the rift (see Fig. 6 in Gao et al. [7]). This feature of LAB is quite consistent with our present result (Figs. 6a and 7a) if we assume that the high-V zone from the Moho down to about 180 km depth represents the lithosphere, although we did not make any assumption about the LAB geometry in our tomographic inversions.

Gao et al. [7] used the ACH method [32] to determine the 3-D velocity structure down to 410 km depth under the Baikal rift zone. Note that they used only 28 stations (dots in Fig. 1) along a 1280-km long, NW–SE oriented profile in their tomographic inversion. Achauer and Masson [12] also applied the ACH method to the same data set to determine tomographic images down to 337 km depth. In plan views, the images of the two previous studies look similar to our present result. However, they did not show their tomographic results in a vertical cross-section in their papers, so it is difficult to compare the present result with theirs in depth views.

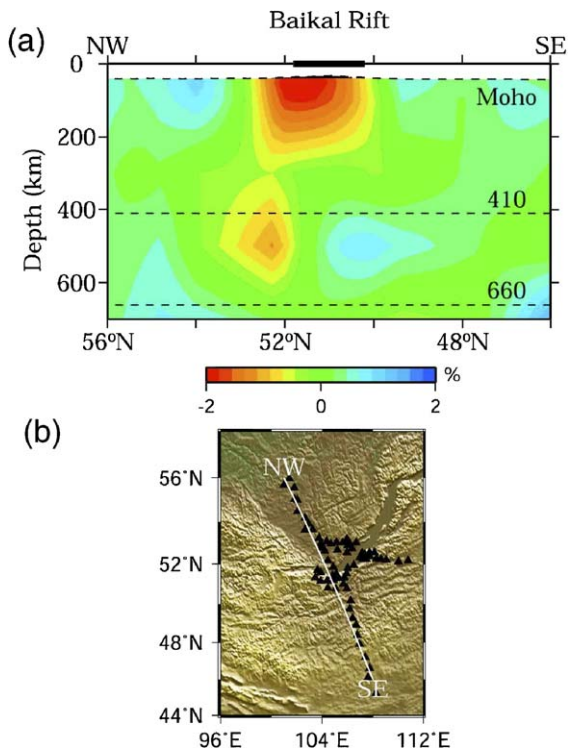


Fig. 6. (a) Vertical cross-section of P-wave velocity image along a profile as shown in panel (b). The model CRUST2.0 [34] was used for the crustal correction. Red and blue colors denote slow and fast velocities, respectively. The velocity perturbation scale is shown below the cross-section. The three dashed lines denote the Moho, 410 and 660km discontinuities. The bold bar at the top of the cross-section denotes the location of the Baikal rift zone. Solid triangles in panel (b) show the locations of seismic stations.

Petit et al. [19] used a large number of lower-quality data from local and teleseismic events to determine the 3-D P-wave velocity structure of a broad region around the Baikal rift zone. An important result of their inversion is that a thin, plume-like, low- V zone is revealed under the southern portion of the Siberian craton down to about 660km depth, and the plume is tilting toward the northwest. Their result is consistent with our present one, although their plume image looks different from that in our tomographic image.

Our tomographic images show that low- V anomalies extend down to the mantle transition zone under the Baikal rift zone (Figs. 6 and 7). If the low- V zones represent a hot upwelling (plume), it is interesting to determine whether this upwelling originates from the 660km discontinuity or from the lower mantle or even the core–mantle boundary. To clarify this problem, we need a future seismic network with a larger aperture to determine the deeper structure under the Baikal region. Receiver function methods can also be used to map the

geometry of the 410 and 660km discontinuities, which can provide information on the origin depth of the upwelling. If the upwelling originates from the lower mantle, then it will cause the 660km discontinuity to be elevated, and the 410km discontinuity to be depressed, resulting in a thinner mantle transition zone (e.g., [37]). A recent receiver function analysis shows that both the 410 and 660km discontinuities deepen from the Baikal rift zone toward the Siberian craton [38]. This suggests that the upwelling under the Baikal rift zone may

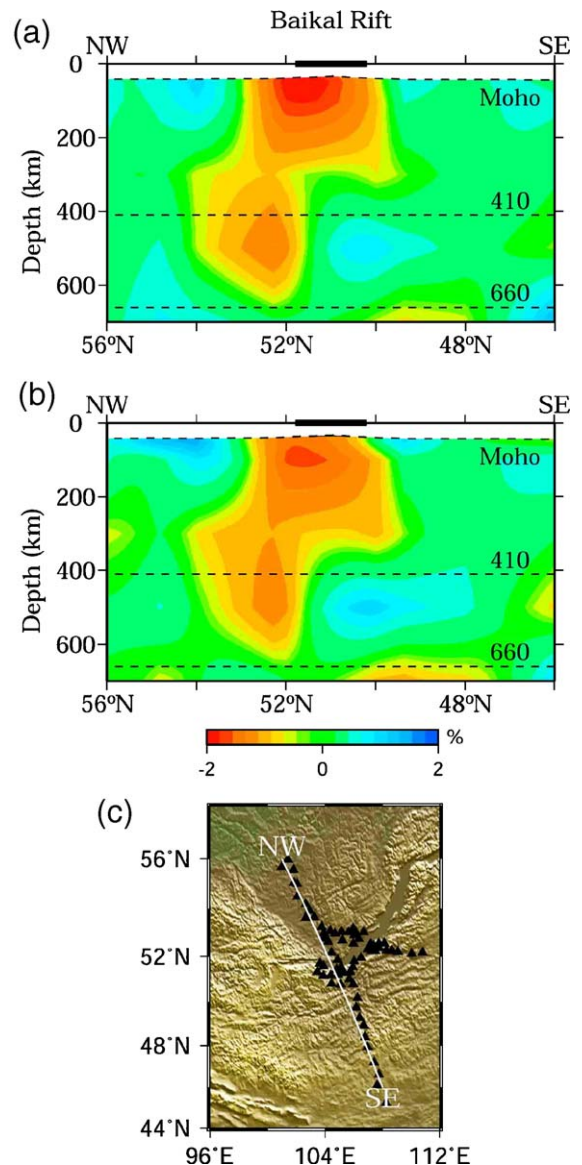


Fig. 7. (a) The same as Fig. 6a but the 3-D crustal model [36] was used for the crustal correction. (b) The result of a synthetic test with the image in (a) as the input model (see text for details). (c) Map showing the location of the cross-sections shown in panels (a) and (b).

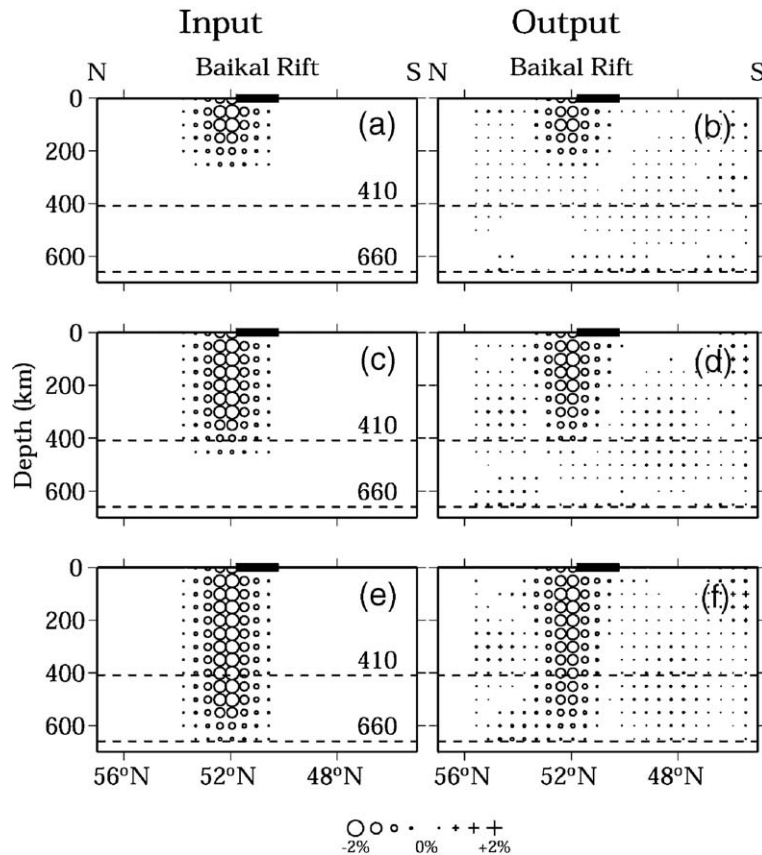


Fig. 8. Input models (left) and inverted results (right) of the synthetic tests conducted (see text for details). Circles and crosses denote slow and fast velocities, respectively. The velocity perturbation scale is shown at the bottom. The bold bar at the top of the cross-sections denotes the location of the Baikal rift zone.

originate beneath the 410 km discontinuity and above the 660 km discontinuity, rather than in the lower mantle, being consistent with the present tomographic result that the low-V zones extend down to 600 km depth and no deeper (Figs. 6 and 7).

The low-V zones under the Baikal rift do not show a simple vertical pillar shape, but a complex and deflected image. Such a result is not surprising if the low-V zones represent a hot upwelling plume. Deflected plumes have been revealed under Iceland, Hawaii, Africa and South Pacific by global tomographic imaging [24,28,39] and receiver function analyses [37]. The existence of deflected plumes in the mantle is also shown by computer simulations, suggesting that plumes can be tilted by the mantle flow [40]. Local structures of the lithosphere such as the edge of the Siberian craton may also affect the route of an upwelling plume, causing its deflection [41].

The Baikal rift basins began to form in the Oligocene (about 30–35 Ma) and they are still developing. Magmatism related to the development of the rift zone

is relatively small in volume. However, most of the volcanics in the rift zone and its vicinity are not much different in chemical composition from volcanics of other continental Cenozoic rift zones [42,43]. Here, olivine tholeiites, alkaline olivine basalts, and hawaiites are predominant. The latter include basanites, olivine melaleucites, and melanephelinites [44]. The geochemical and isotopic data from the basalt fields in the Baikal rift zone indicate that mantle plumes could be the source of these volcanics [6,45,46]. Although the major volcanic activity took place in the late Oligocene–Quaternary period (i.e., during the rift zone development), the earliest volcanism in the Baikal region occurred in the Latest Cretaceous–Paleocene (80–35 Ma), i.e., at a time when the rift zone did not yet exist [44]. This fact was taken as strong evidence for the existence of mantle plume(s) in the region, and was considered as a typical feature of active rifting [6]. The last volcanic episodes occurred here about 2–10 ka ago [44].

Mantle plumes seem to be the main cause of the Baikal rift zone, but they are not sufficient for rifting [6].

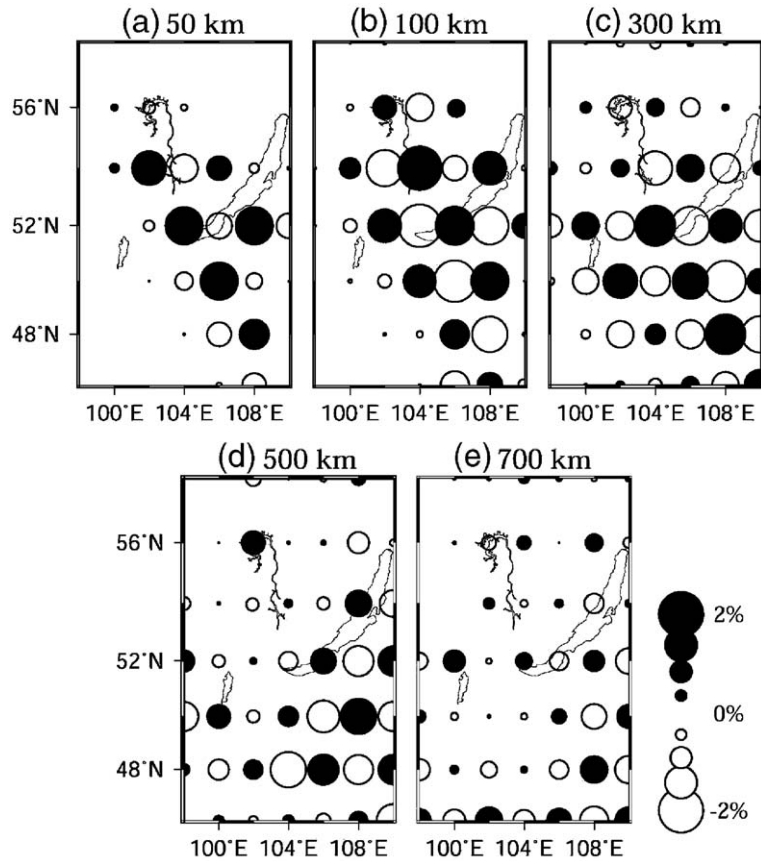


Fig. 9. Results of a checkerboard resolution test (see text for details). Open and solid circles denote slow and fast velocities, respectively. The velocity perturbation scale is shown on the right. The layer depth is shown above each map.

It was suggested that the combination of three conditions was necessary for the development of the rift zone: (1) mantle plumes, (2) older (prerift) linear lithosphere structures favorable in position relative to the plumes, and (3) favorable orientation of the far-field forces provided by the India–Asia collision [6,13–15]. These are the same conditions as those suggested for other Cenozoic continental rifts (Kenya, Rio Grande, and Rhine) although a different order of the listed causes was considered [12].

In this study we could only determine the structure under the western portion of the Baikal rift zone because of the location of the available seismic stations. It is important to know whether a similar structure exists under other parts of the broad Baikal rift zone. In future investigations, portable seismic stations should be deployed to cover the eastern and central parts of the rift zone, which will enable us to determine the deep structure under the entire rift zone to clarify its origin and evolutionary processes.

5. Conclusions

We determined a detailed 3-D P-wave velocity structure of the upper mantle beneath the Baikal rift zone using a large number of high-quality arrival time data collected from original seismograms of teleseismic events recorded by a dense portable seismic network. Low-velocity anomalies in the upper mantle with a lateral velocity reduction of up to 2% are revealed under the Baikal rift zone. The low-velocity feature extends from the surface down to the mantle transition zone and tilts toward the northwest under the stable Siberian craton. It is interpreted as a mantle upwelling (plume) which has played an important role in the initiation and evolution of the Baikal rift zone. The lithosphere of the stable Siberian craton is imaged as a high-velocity anomaly having a thickness of 150–180 km. Strong lateral heterogeneity exists in the lithosphere of the complex Mongolian fold belt. In addition to the dominant role of the Baikal mantle plume, the rift

formation may also be controlled by other factors such as older (prerift) linear lithosphere structures favorably positioned relative to the plume and favorable orientation of the far-field forces caused by the India–Asia collision.

Acknowledgments

This work was partially supported by grants (Kiban-B 11440134, and Kiban-A 17204037) from the Japan Society for the Promotion of Science and a special grant for the Center of Excellence (COE) from Ehime University to D. Zhao and A. Yamada. The figures are made by using GMT [47]. S. King, J. Nakajima and two anonymous referees provided constructive review comments that improved the manuscript.

References

- [1] P. Molnar, P. Tapponnier, Cenozoic tectonics of Asia: effects of a continental collision, *Science* 189 (1975) 419–426.
- [2] N. Logatchev, N. Florensov, The Baikal system of rift valleys, *Tectonophysics* 45 (1978) 1–13.
- [3] L. Zonenshain, L. Savostin, Geodynamics of the Baikal rift zone and plate tectonics of Asia, *Tectonophysics* 76 (1981) 1–45.
- [4] S. Gao, P. Davis, K. Liu, P. Slack, Y. Zorin, N. Logatchev, M. Kogan, P. Burkholder, R. Meyer, Asymmetric upwarp of the asthenosphere beneath the Baikal rift zone, Siberia, *J. Geophys. Res.* 99 (1994) 15319–15330.
- [5] Y. Zorin, L. Cordell, Crustal extension in the Baikal rift zone, *Tectonophysics* 198 (1991) 117–121.
- [6] Y. Zorin, E. Turutanov, V. Mordvinova, V. Kozhevnikov, T. Yanovskaya, A. Treussov, The Baikal rift zone: the effect of mantle plumes on older structure, *Tectonophysics* 371 (2003) 153–173.
- [7] S. Gao, K. Liu, P. Davis, P. Slack, Y. Zorin, V. Mordvinova, V. Kozhevnikov, Evidence for small-scale mantle convection in the upper mantle beneath the Baikal rift zone, *J. Geophys. Res.* 108 (2003) 2194.
- [8] D. Doser, Faulting within the western Baikal rift as characterized by earthquake studies, *Tectonophysics* 196 (1991) 87–107.
- [9] Y. Zorin, V. Kozhevnikov, M. Novoselova, E. Turutanov, Thickness of the lithosphere beneath the Baikal rift zone and adjacent regions, *Tectonophysics* 168 (1989) 327–337.
- [10] A. Kiselev, A. Popov, Asthenospheric diapir beneath the Baikal rift: petrological constraints, *Tectonophysics* 208 (1992) 287–295.
- [11] A. Yin, Mode of Cenozoic east–west extension in Tibet suggesting a common origin of rifts in Asia during the Indo-Asian collision, *J. Geophys. Res.* 105 (2000) 21745–21760.
- [12] U. Achauer, F. Masson, Seismic tomography of continental rifts revisited: from relative to absolute heterogeneities, *Tectonophysics* 358 (2002) 17–37.
- [13] C. Petit, J. Deverchere, F. Houdry, V. Sankov, V. Melnikova, D. Delvaux, Present-day stress field changes along the Baikal rift and tectonic implications, *Tectonics* 15 (1996) 1171–1191.
- [14] D. Delvaux, R. Moeys, G. Stapel, C. Petit, K. Levi, Paleostress reconstructions and geodynamics of the Baikal region, central Asia: Part II. Cenozoic rifting, *Tectonophysics* 282 (1997) 1–38.
- [15] O. Lesne, E. Calais, J. Deverchere, J. Chery, R. Hassani, Dynamics of intracontinental extension in the north Baikal rift from two-dimensional numerical deformation modeling, *J. Geophys. Res.* 105 (2000) 21727–21744.
- [16] N. Puzyrev, M. Mandelbaum, S. Krylov, B. Mishenkin, G. Petrik, G. Krupskaya, Deep structure of the Baikal and other continental rift zones from seismic data, *Tectonophysics* 45 (1978) 87–94.
- [17] A. Popov, A deep geophysical study in the Baikal region, *Pure Appl. Geophys.* 134 (1990) 575–587.
- [18] S. Gao, P. Davis, K. Liu, P. Slack, A. Rigor, Y. Zorin, V. Mordvinova, V. Kozhevnikov, N. Logatchev, SKS splitting beneath continental rift zones, *J. Geophys. Res.* 102 (1997) 22781–22797.
- [19] C. Petit, I. Koulakov, J. Deverchere, Velocity structure around the Baikal rift zone from teleseismic and local earthquake traveltimes and geodynamic implications, *Tectonophysics* 296 (1998) 125–144.
- [20] E. Engdahl, R. van der Hilst, R. Buland, Global teleseismic earthquake location with improved travel times and procedure for depth determination, *Bull. Seismol. Soc. Am.* 88 (1998) 722–743.
- [21] B. Kennett, E. Engdahl, Traveltimes for global earthquake location and phase identification, *Geophys. J. Int.* 105 (1991) 429–465.
- [22] D. Zhao, A. Hasegawa, Teleseismic evidence for lateral heterogeneities in the northeastern Japan arc, *Tectonophysics* 237 (1994) 189–199.
- [23] D. Zhao, A. Hasegawa, H. Kanamori, Deep structure of Japan subduction zone as derived from local, regional, and teleseismic events, *J. Geophys. Res.* 99 (1994) 22313–22329.
- [24] D. Zhao, Seismic structure and origin of hotspots and mantle plumes, *Earth Planet. Sci. Lett.* 192 (2001) 251–265.
- [25] D. Zhao, A. Hasegawa, S. Horiuchi, Tomographic imaging of P and S wave velocity structure beneath northeastern Japan, *J. Geophys. Res.* 97 (1992) 19909–19928.
- [26] D. Zhao, J. Lei, Seismic ray path variations in a 3-D global velocity model, *Phys. Earth Planet. Inter.* 141 (2004) 153–166.
- [27] C. Paige, M. Saunders, LSQR: an algorithm for sparse linear equations and sparse least squares, *ACM Trans. Math. Softw.* 8 (1982) 43–71.
- [28] D. Zhao, Global tomographic images of mantle plumes and subducting slabs: insight into deep Earth dynamics, *Phys. Earth Planet. Inter.* 146 (2004) 3–34.
- [29] J. Lees, R. Crosson, Tomographic inversion for three-dimensional velocity structure at Mount St. Helens using earthquake data, *J. Geophys. Res.* 94 (1989) 5716–5729.
- [30] H. Inoue, Y. Fukao, K. Tanabe, Y. Ogata, Whole mantle P wave travel time tomography, *Phys. Earth Planet. Inter.* 59 (1990) 294–328.
- [31] S. Hung, Y. Shen, L. Chiao, Imaging seismic velocity structure beneath the Iceland hot spot: a finite frequency approach, *J. Geophys. Res.* 109 (2004) B08305.
- [32] K. Aki, A. Christofferson, E. Husebye, Determination of the three-dimensional seismic structure of the lithosphere, *J. Geophys. Res.* 82 (1977) 277–296.
- [33] J. Lei, D. Zhao, P-wave tomography and origin of the Changbai intraplate volcano in Northeast Asia, *Tectonophysics* 397 (2005) 281–295.
- [34] G. Laske, G. Masters, C. Reif, CRUST2.0: A new global crustal model at 2°×2 degrees, <http://mahi.ucsd.edu/Gabi/rem.dir/crust/crust2.html>.

- [35] W. Mooney, G. Laske, G. Masters, CRUST 5.1: a global crustal model at 5×5 degrees, *J. Geophys. Res.* 103 (1998) 727–747.
- [36] S. Gao, K. Liu, C. Chen, Significant crustal thinning beneath the Baikal rift zone: new constraints from receiver function analysis, *Geophys. Res. Lett.* 31 (2004) L20610.
- [37] Y. Shen, S. Solomon, I. Bjarnason, G. Nolet, Seismic evidence for a tilted mantle plume and north–south mantle flow beneath Iceland, *Earth Planet. Sci. Lett.* 197 (2002) 261–272.
- [38] T. Inoue, J. Lei, A. Yamada, D. Zhao, S. Gao, Upper mantle structure under the Baikal rift zone derived from receiver function analyses, *Earth Monthly* 27 (2005) 773–776.
- [39] H. Bijwaard, W. Spakman, Tomographic evidence for a narrow whole mantle plume below Iceland, *Earth Planet. Sci. Lett.* 166 (1999) 121–126.
- [40] B. Steinberger, Plumes in a convecting mantle: models and observations for individual hotspots, *J. Geophys. Res.* 105 (2000) 11127–11152.
- [41] S. King, J. Ritsema, African hot spot volcanism: small-scale convection in the upper mantle beneath cratons, *Science* 290 (2000) 1137–1140.
- [42] N. Logatchev, Y. Zorin, V. Rogozhina, Baikal rift: active or passive? Comparison of the Baikal and Kenya rift zones, *Tectonophysics* 94 (1983) 223–240.
- [43] P. Lipman, N. Logatchev, Y. Zorin, C. Chapin, V. Kovalenko, P. Morgan, Intracontinental rift comparison: Baikal and Rio Grande rift systems, *Eos Trans. AGU* 70 (1989) 578–588.
- [44] S. Rasskazov, Magmatism related to Eastern Siberia rift system and the geodynamics, *Bulletin des Centres de Recherches Exploration – Production Elf Aquitaine* 18 (1994) 437–452.
- [45] V. Yermolyuk, V. Kovalenko, V. Ivanov, Intraplate Late Mesozoic–Cenozoic volcanic province in Central–Eastern Asia as projection of mantle hot field (in Russian), *Geotektonika* 5 (1995) 41–64.
- [46] A. Grachev, The Khamardaban Ridge as a hotspot of the Baikal rift from data of chemical geodynamics, *Phys. Solid Earth* 34 (1998) 175–200.
- [47] P. Wessel, W. Smith, New, improved version of the Generic Mapping Tools released, *Eos Trans. AGU* 79 (1998) 579.